Accepted Manuscript

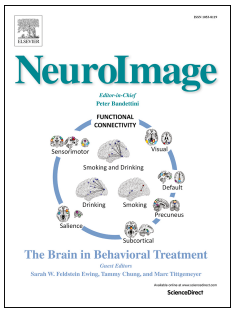

High frequency neurons determine effective connectivity in neuronal networks

Aref Pariz, Zahra G. Esfahani, Shervin S. Parsi, Alireza Valizadeh, Santiago Canals, Claudio R. Mirasso

PII: S1053-8119(17)30921-7

DOI: 10.1016/j.neuroimage.2017.11.014

Reference: YNIMG 14461

To appear in: *NeuroImage*

Received Date: 6 July 2017

Revised Date: 31 October 2017

Accepted Date: 5 November 2017

Please cite this article as: Pariz, A., Esfahani, Z.G., Parsi, S.S., Valizadeh, A., Canals, S., Mirasso, C.R., High frequency neurons determine effective connectivity in neuronal networks, *NeuroImage* (2017), doi: 10.1016/j.neuroimage.2017.11.014.

This is a PDF file of an unedited manuscript that has been accepted for publication. As a service to our customers we are providing this early version of the manuscript. The manuscript will undergo copyediting, typesetting, and review of the resulting proof before it is published in its final form. Please note that during the production process errors may be discovered which could affect the content, and all legal disclaimers that apply to the journal pertain.

ACCEPTED MANUSCRIPT

High frequency neurons determine effective connectivity in neuronal networks

Aref Pariz[a,b], Zahra G. Esfahani[b], Shervin S. Parsi[a], Alireza Valizadeh[a,b], Santiago Canals[c], Claudio R. Mirasso[d,*]

[a] *Institute for Advanced Studies in Basic Sciences, Zanjan, Iran*
[b] *School of Cognitive Sciences, Institute for Research in Fundamental Sciences, Tehran, Iran*
[c] *Instituto de Neurociencias, Consejo Superior de Investigaciones Científicas, Universidad Miguel Hernández, Sant Joan d'Alacant 03550, Spain*
[d] *Instituto de Física Interdisciplinary Sistemas Complejos IFISC (UIB-CSIC), Campus Universitat de les Illes Balears, 07122 Palma de Mallorca, Spain*

Abstract

The emergence of flexible information channels in brain networks is a fundamental question in neuroscience. Understanding the mechanisms of dynamic routing of information would have far-reaching implications in a number of disciplines ranging from biology and medicine to information technologies and engineering. In this work, we show that the presence of a node firing at a higher frequency in a network with local connections, leads to reliable transmission of signals and establishes a preferential direction of information flow. Thus, by raising the firing rate a low degree node can behave as a functional hub, spreading its activity patterns polysynaptically in the network. Therefore, in an otherwise homogeneous and undirected network, firing rate is a tunable parameter that introduces directionality and enhances the reliability of signal transmission. The intrinsic firing rate across neuronal populations may thus determine preferred routes for signal transmission that can be easily controlled by changing the firing rate in specific nodes. We show that the results are generic and the same mechanism works in the networks with more complex topology.

*Corresponding author

ACCEPTED MANUSCRIPT

Introduction

How does the brain integrate the multiplicity of local processes dispersed through its entire extent? Complex network analysis of brain activity recorded with functional magnetic resonance imaging (fMRI) or electroencephalography (EEG) suggests the existence of influential nodes in the network with a prominent role in integration (Sporns (2014)). Several topological properties have been suggested to define highly influential nodes, the most important being the "hub-nodes", i.e., nodes (brain regions) with a disproportionately large number of connections to other parts of the brain. Network hubs have been hypothesized to play a crucial role not only in the integrity of the normal brain but also in disease states (van den Heuvel and Sporns (2013)). For instance, disruption in hub nodes and their connections have been proposed as a hallmark for Alzheimer's disease (Buckner et al. (2009), schizophrenia (Fornito et al. (2012)), and disorders of consciousness (Achard et al. (2012)).

In contrast to other complex networks, in the nervous system dynamic functional connections ride on top of the anatomical structure, providing resiliency to the communication channels hardwired in the network topology (Friston (2011); Fries (2005, 2015)). Therefore, the influence of a node does not only depend on its degree and position in the network ((Amit and Tsodyks (1992); Zbinden (2011)) but importantly also on its internal dynamics. The fundamental functional characteristic of such dynamic networks is that the set of nodes and links that critically define activity propagation in the system can be optimized independently for different contexts or tasks, resulting in diverse network configurations and providing flexibility. This optimization, in the case of the nervous system, needs to expand across orders of magnitude in temporal and spatial scales to accommodate the diversity of neural processing ((Park and Friston (2013); Logothetis (2012)).

In the present paper, we study activity propagation in networks with local connections and homogeneous topology when inhomogeneities are introduced in the dynamical characteristics of the constituent nodes. To this end, we consider

ACCEPTED MANUSCRIPT

a mutually-coupled network where each node represents a unit composed of excitatory and inhibitory neurons. In our study, all nodes except one, produce a local oscillation with frequency ν_0 in the gamma range. An inhomogeneity is introduced in the network by placing the remaining node –*source node*– to oscillate at a different intrinsic frequency $\nu = \nu_0 + \Delta\nu$, in the otherwise homogeneous ensemble. To assess the network response to local inputs, we first perturb the system with a signal superimposed on one of the nodes and then we use a generalization of the phase response curve (PRC) for the network (Kawamura et al. (2008)). Network PRC (nPRC) is defined as the average change of the period T of the mean firing activity of the network due to a local perturbation. We find that long-range influences of the local perturbation are facilitated when the node that receives the perturbation has a higher intrinsic frequency as compared to the rest of the nodes. In the second part of the study, we examine the implications of this result in the propagation of signals in the networks. To this end, we superimpose a periodic input over one of the nodes and test the maximum of the power spectrum of all the nodes at the frequency of the external signal. We find, for modulation frequencies higher than ν_0, a constructive role of the inhomogeneity in the propagation of the signal through the network. Interestingly, this mechanism is generic and works for highly heterogeneous and complex topologies including CoCoMac connectome network. The presence of high frequency nodes can be crucial for the propagation of signals in networks with local connections. With this simple mechanism, we propose a model to explain how complex networks with fixed anatomical structures can generate a multiplicity of functional states.

Material and Methods

Neuron's and synaptic model. The neurons are modeled as leaky Integrate-fire (LIF) model which is described by the first order differential equation (Burkitt (2006))

$$\tau_i \frac{dv_i}{dt} = -(v_i - v_{leak}) + I_i + \eta_i(t) + \sum_j I_{ij}(t) + J_i(t), \qquad (1)$$

ACCEPTED MANUSCRIPT

where v_i is the membrane potential of the neuron i and v_{leak} is the leak membrane potential. I_i is a constant bias current, η_i is an independent Gaussian white noise current with zero mean and standard deviation σ impinging neuron i, I_{ij} represents the synaptic current from neuron j to i and $J_i(t)$ accounts for a local current signal. Every time the membrane potential exceeds a threshold potential v_{th}, the neuron *spikes* and the potential resets to a resetting potential v_{res}, and is clamped at this potential for 0.5 ms as the absolute refractory period. The membrane time constant τ_i is equal to $C_m R_m$ where C_m and R_m are the capacitance and the resistance of the membrane, respectively. While the inputs appear as currents, they are measured in units of the membrane potential (mV) because a factor of the membrane resistance has been absorbed into their definition (Babadi and Abbott (2013)). Assuming a reasonable value for the membrane resistance, e.g. $R_m = 100$ MΩ, a voltage of 1 mV translates to a current of 10 pA in the standard units (Bayati and Valizadeh (2012)). The synaptic current is described as

$$I_{ij}(t) = a_{ij} g_{ij} \sum_k \delta(t - t_j^k) \tag{2}$$

where a_{ij} characterizes the connectivity and is equal to 1 if two neurons i, j are connected; otherwise $a_{ij} = 0$. g_{ij} is the efficacy of the synapse from neuron j to neuron i. In the simulations we have taken the resetting potential $v_{res} = 0$ mV and the threshold $v_{thr} = 10$ mV. The membrane time constants of the neurons are chosen from a uniform random distribution with mean 10 ms and standard deviation 0.1 ms (Cortes and Vreeswijk (2015)). Input current to each neuron is taken $I_0 = 11$ mV with $\sigma = 0.1$ mV unless otherwise noted. To integrate the equation 1 with the synaptic currents given by equation 2 we use the Milshtein algorithm with a time step of 0.1 ms. All the simulations were carried out in MATLAB environment.

Structure of the network. We construct a chain of N nodes, each consisting of 80 excitatory (E) and 20 inhibitory (I) neurons (see Figure 1). Within the nodes, the connections between excitatory and inhibitory neurons are chosen with probabilities $p_{EE} = p_{II} = p_{EI} = p_{IE} = p_{in} = 0.1$ (E stands for

ACCEPTED MANUSCRIPT

excitatory and I for inhibitory and the first and second letters in subscript denote the presynaptic and postsynaptic neurons, respectively). Between nodes, only excitatory neurons of adjacent populations are mutually connected with probability $p_{ext} = 0.1$. Excitatory synaptic strengths are chosen all equal to 0.2 mV (except when we vary them) while inhibitory connections are equal to 0.8 mV. The delay in the connections between neurons in the same network is taken 0.5 ms and between the neurons of neighboring networks 1 ms. In the results presented in Fig. 9 we use two other topologies: a ring in which the first node is connected to N^{th}-node, and a starlike topology in which one of the nodes is connected to several other nodes as is schematically shown in Fig. 9 (c and d). As the final example, we test the validity of our results in a biologically realistic structure extracted from CoCoMac connectome data (available at the Brain Connectivity Toolbox, https://sites.google.com/site/bctnet/) whose characteristics are depicted in Fig. 10.

Network response to local signals. To quantify the response of the network to the local external signals, we use the network phase resetting curve (nPRC), as a generalization of the PRC notion for single neurons. This quantity measures the average change in the oscillation phase of the nodes, due to the impact of a pulse to one of the nodes (host) in the network. In other words, nPRC is a measure on how the collective activity of a node is influenced by a pulse imposed on the same node, or on the other nodes. To calculate nPRC we first run a simulation for the unperturbed system and calculate the firing rate of each node with a Gaussian time window of the width 4 ms. Then we apply a weak pulse to all the excitatory neurons in a node, keeping the rest of the network parameters fixed, and using the same input noise to all the neurons (noise is frozen in the two simulations). The time interval between two consecutive peaks of the network oscillation of the host node is divided into 0.5 ms time bins. A pulse of duration 2 ms and amplitude 0.25 mV is imposed on all excitatory neurons of the host node. Then, by calculating the firing rate of each node, and subtracting the period before and after the application of the pulse, we calculate the PRC of each node. By taking the mean change of

ACCEPTED MANUSCRIPT

the period of all the nodes for each pulse, the nPRC of the whole network is calculated.

To further study the propagation of local external signals along the network, we apply a periodic signal $J(t) = A\ \sin(2\pi ft)$ to all of the excitatory neurons of the host node. The response of the individual nodes is calculated in two ways: In both the methods we first calculate the network activity for each node by convolving the firing activity of the node with a Gaussian window of 50 ms width. Then the first response measure is defined as the maximum of the power spectrum of the network activity at the frequency of the external signal. In the second method, we take the cross-covariance of the network activity with the external signal for different nodes.

Then, two signals with different frequencies are simultaneously imposed on two different nodes to compare their propagation in the network and infer the effective connectivity and the response, as described above, is measured to probe the propagation of the two signals through the network.

Information transfer and effective connectivity. Effective connectivity is formally defined based on the causal relationship between the activity of the nodes in a network. We hypothesize that the notion of effective connectivity has a close relationship with the transmission of local signals in the network. To detect a causal relationship between the dynamics of two nodes, we used time-delayed mutual information (δMI) which quantifies the directionality of the information flow between every two nodes of the network Kirst et al. (2016). In this method, the activity of one neuronal population shifted by a time lag d is compared with the instantly recorded neuronal activity of another population. Delayed mutual information is defined based on the Shannon's formula for discrete time-series

$$\begin{aligned} \delta MI_{i,j}(d) &= \delta MI(X_i(t), X_j(t+d)) \\ &= H(X_i(t)) + H(X_j(t+d)) - H(X_i(t), X_j(t+d)), \end{aligned}$$

where $H(X_i(t))$ is the marginal entropy of series X_i, computed using the stan-

ACCEPTED MANUSCRIPT

dard definition

$$H(X_i) = -\sum_{k \in X_i} P_k \log(P_k)$$

where *log* is logarithm to the base 2, P_k is the probability of occurrence of kth position at discretized series $X_i(t)$, and $H(X_i(t), X_j(t+d))$ is the joint entropy of X_i and X_j, where the latter is time-shifted by d

$$H(X_i(t), X_j(t+d)) = -\sum_{n \in X_i(t)} \sum_{m \in X_j(t+d)} P_{n,m} \log(P_{n,m}).$$

Here $P_{n,m}$ is the joint probability of nth and mth positions occurring together at discretized series $X_i(t)$ and $X_j(t+d)$, respectively. Integrating delayed mutual information for positive lags measures the MI transferred from the i^{th} population to the j^{th} one ($MI_{i\to j} = \int_0^\infty \delta MI_{i,j}(d')\ dd'$), and integration over the negative lags quantifies the MI flow in the reverse direction ($MI_{j\to i} = \int_{-\infty}^0 \delta MI_{i,j}(d')\ dd'$). Subtracting these two values gives the preferred direction of the information flow ($\delta MI_{i,j} = MI_{i\to j} - MI_{j\to i}$), and the direction of the connection in the effective network.

Results

We consider a network consisting of $N = 11$ nodes (or nodes) where each node is composed of 80 excitatory and 20 inhibitory neurons sparsely connected with probability 0.1. Excitatory neurons of adjacent nodes are connected via current-based excitatory synapses with probability 0.1 (Figure 1). The dynamics of the neurons is described by the leaky integrate-fire (LIF) model. The external current and intra-node connections are set such that all the nodes, except one (source node), produce an internal rhythm in the gamma range ($\nu_0 \simeq 42$ Hz) when isolated, i.e., when inter-node connections are absent (see Figure 2). Heterogeneity in the network is introduced by changing the external current to the excitatory neurons of one of the nodes by an amount ΔI, which in this case and without loss of generality, is chosen as the middle node (node 6). By changing ΔI we can control the oscillation frequency ν of the middle

ACCEPTED MANUSCRIPT

node as is shown in Figure 2d. Results obtained with conductance-based models are qualitatively similar (see Supplementary Information). Moreover, we have checked that changes in the proportion of excitatory-inhibitory neurons and the strength of the internal connectivity do not qualitatively alter our findings.

Response function of the network

When the nodes are connected by excitatory synapses, they all oscillate with the same frequency (i.e., the nodes fall into the $1:1$ frequency locking regime) if the inhomogeneity ΔI is small (Figure 2). To infer the response of the system to local inputs, we perturb the network by injecting a weak current pulse into all the excitatory neurons of one of the nodes (*host node*) at a time τ, or equivalently at a phase ϕ defined as $\phi = 2\pi\frac{\tau}{T}$ (where T is the period of the network oscillation), between two consecutive peaks of the oscillations of the host node. We vary ϕ over 2π and evaluate the response of the whole network which is defined as the mean change in the oscillation period of all the nodes due to the application of the current pulse (see Material and Methods).

To highlight the role of the high-frequency node in shaping the response of the system to a local input, we change the host node into which the pulse is injected. Initially, we test a homogeneous system, where all the nodes have almost the same intrinsic frequency ν_0, and then a heterogenous network containing a high frequency node. As shown in Figure 3a, in the homogeneous network ($\Delta\nu = 0$) the response function is independent, as expected, of the node on which the pulse is applied. Moreover, the response is negligibly small regardless of the phase at which the pulse is applied and the location of the host node. On the contrary, in the presence of a high-frequency node, the response critically depends on the node at which the current pulse is applied. The response considerably increases when the pulse is applied on the high-frequency node and sharply decays when it is applied progressively away from it. So, the presence of a high-frequency node not only creates an inhomogeneity in the spatial response of the system, but also increases the sensitivity of the system to local perturbations which are imposed on, or in the vicinity of, the source node.

ACCEPTED MANUSCRIPT

We then test how the response of the system changes with the level of inhomogeneity and the inter-node connection strength, to find the optimum range of parameters that maximizes the system response. To this end, we impose a short current pulse on the high-frequency node at the oscillation phase around which the response of the system is maximum ($\simeq 3\pi/2$ as can be seen in Figure 3). In Figure 4 it is shown how the response changes for increasing values of $\Delta\nu$ (due to the changes ΔI in the input current) of the source node for different values of inter-node connection strength g_{IN}. We find that by increasing the source node's intrinsic oscillation frequency by $\Delta\nu$, the mean response initially increases and then gradually decreases. A qualitatively similar trend is seen in the signal-to-noise ratio (SNR), defined as the ratio of the mean response to the standard deviation of the response due to the trial-to-trial variability. The two measures indicate that there is an optimum range of $\Delta\nu$ for which the response is the largest and most reliable. Both the response and the signal-to-noise ratio are maximized for intermediate strength of inter-node connections g_{IN} (see right panels of Figure 4).

Signal propagation in the network

In this section, we show that the presence of a high-frequency node also facilitates the propagation of local signals. To this end, a slowly-varying periodic signal is injected into all the excitatory neurons of the middle node. Then the network response is evaluated as the value of the power spectrum of the activity of the nodes at the frequency of the external signal. Also, the cross-covariance of the node activities and the external signal is calculated (see Material and Methods). In Figure 5 (a and b) it can be seen, for an input signal of frequency $f_0 = 4$ Hz, how the activity of one node (in this case node 10) and its power spectrum change with the oscillating frequency of the host node (node 6). An optimum response, accompanied with a maximum in the power spectrum, is observed for $\Delta\nu = 4.8$ Hz, i.e., when the oscillation frequency of the host node is $\nu = 46.8$ Hz. The response rapidly increases from $\Delta\nu = 0$ and slowly decreases for $\Delta\nu \gtrsim 7$ Hz. The maximum response of the different nodes is also plotted

ACCEPTED MANUSCRIPT

in Figure 5c versus the inhomogeneity parameter $\Delta\nu$. It can be seen that the response increases until a maximum value is reached around $\Delta\nu = 5$ Hz. This large response maintains for a relatively wide range of $\Delta\nu$, which does not depend much on the coupling strength (see Figure 5c). It is worth noting, also in Figure 5c, that negative values of $\Delta\nu$, which result in a lower oscillation frequency of the host node, decrease the response of the network. This result indicates that activity propagation in this system can be regulated (enhanced or depressed) through the same mechanism, this is, by controlling the firing rate in the host node.

To check if the increase of the network response is a result of a resonance of the external signal with the internal frequency of the network, we vary the frequency f_0 of the external signal and record the response of the network. It can be seen in Figure 5d that when varying f_0, the maximum response stays around $\Delta\nu = 5$. However, its maximum value decreases almost linearly with the input frequency indicating that slower signals are better amplified than faster ones. The results rule out a resonant behavior and show a low-pass filter-like behavior where slow varying signals can better propagate along the network by modulating the firing rate of the populations (Figure 5d). It is worth noting that the periodicity of the external signal is not a criterion of validity of the results; any slowly varying non-periodic signals yield similar behavior as is shown in Supplementary Fig. S1.

For the sake of a better illustration in Figure 6 we show the mean firing rate of the 11 nodes for different values of the inhomogeneity parameter $\Delta\nu$, when a signal of frequency $f_0 = 4$ Hz is injected into node 6. It is evident that for intermediate values of the inhomogeneity parameter the signal better propagates along the whole network. For $\Delta\nu = 4.8$ Hz the input signal clearly reaches both sides of the network. For other values of $\Delta\nu$ the signal does not propagate (panel a and d) or propagates just weakly (panel c).

ACCEPTED MANUSCRIPT

Information transfer and effective feed-forward connectivity

The results presented in the previous sections suggest that the propagation of an external pulse or signal through the network is facilitated if the host node oscillates at a higher frequency as compared to the other nodes. Therefore, despite the homogeneous symmetric connections, the presence of a high frequency node establishes a preferred feedforward direction for the signal transmission. To reveal this *effective connectivity* in a complementary way, we inject two periodic signals in two different nodes of the network. Without loss of generality, we apply a signal of frequency $f_1 = 4.5$ Hz on node 5, which oscillates at a higher frequency, and a signal of frequency $f_2 = 6.5$ Hz on node 7, which oscillates at frequency $\approx \nu_0$.

Figure 7 shows the activity of the network when these two signals are applied simultaneously. In Figure 7a the power spectra of the mean activity of nodes 2 and 10 can be seen. Since the two signals arrive at node 10, a double peak in the power spectrum is observed. On the contrary, node 2 exhibits only one peak at the frequency of the signal injected into node 5. This indicates that the signal injected into node 7 does not reach node 2. These results confirm that the signal propagates only in a preferential direction, moving away from the high frequency node.

In Figure 7b we plot the value of the power spectrum of all nodes at frequencies 4.5 Hz and 6.5 Hz. While the signal applied to the source node elicits response in all nodes, the signal applied to the low frequency node only influences those nodes that are located in the direction away from the high frequency node.

Since the response of the network also depends on the frequency of the external input (Figure 5d), we compute the network response while changing the frequency of the signals applied to nodes 5 and 7. Results depicted in Figures 7c and d show qualitatively similar results as those of Figures 7a and b, highlighting that the frequency of the input signal does not play any role in establishing effective connectivity directions.

In order to directly measure information transfer in the network, we further

ACCEPTED MANUSCRIPT

compute the time-delayed mutual information (δMI), as explained in the Material and Methods. The total information transfer from node i (j) to node j (i) is determined by the integral of the δMI for positive (negative) delay times. The difference between these two integrals gives the direction and strength of the effective link between the two nodes (see Material and methods). The results shown in Fig. 8 (see also Supplementary Fig. S3) further demonstrate that information transfer takes a preferential direction in the presence of a high a frequency node.

From these observations, we conclude that: (i) nodes oscillating with a higher frequency can broadcast their incoming signals throughout the network and (ii) introduce a preferential directionality in the propagation of signals in parallel channels. This occurs despite the symmetric bidirectional nature of the connectivity between nodes and sets effective connectivity channels in the system as is shown in Figs. 7 and 8).

Robustness of the results across network topologies

Although networks have been extensively used as basic structures in sensory systems (Fukushima (2013)), it remains to be demonstrated that the results obtained so far apply to different network topologies. In this section, we extend our study to larger chains and different topologies and evaluate the response of the system to multiple signals imposed on different nodes, similar to what we did in the previous section. For simplicity, we show only results for a detuning $\Delta\nu$ =7.4 Hz for which the response of the network is optimal.

We first increase the number of nodes in the chain to check if the obtained results hold for larger networks (in this case $N = 31$ nodes). The results shown in Fig. 9a indicate that an increasing number of nodes does not qualitatively change the response of the network to the external inputs.

In a second test, we consider a ring structure with $N = 11$ nodes, to check whether our previous observations are altered in the closed network. Results shown in Fig. 9b are qualitatively similar to those obtained for the chain. In both Fig. 9a and b it is clear that the presence of a high frequency node facilitates

ACCEPTED MANUSCRIPT

activity propagation in the network when the input signal is applied to this node.

We next check whether the results also hold true in a network with heterogeneous topology, i.e., with nodes that have a different number of links. In these topologies, nodes with a higher degree (structural hubs) are expected to have maximum influence on the other nodes (Barabási and Albert (1999)). We consider a network combining a starlike structure and a chain (see Fig. 9 insets). In this topology, there is a structural hub whose degree is larger than those of the other nodes in the network. Initially, we assume the hub (node 6) to be a high frequency node and evaluate the propagation of two different signals applied simultaneously to nodes 6 and 8. As shown in Fig. 9c), the signal applied to node 6 clearly transmits to all nodes of the network, as expected, while the signal applied to node 8 is blocked by the high frequency node 6. Interestingly, when a node different to the structural hub is the high-frequency node, the signal applied to the latter propagates through the whole network, while the signal applied to node 6 does not. This indicates that the dynamical effect predominates over the network structure containing a hub. Our results suggest that low degree but high frequency nodes could work as network hubs for information transmission. We refer to them as functional hubs.

The 47 nodes CoCoMac connectome

As a final example, we use the 47 nodes CoCoMac connectome network (available at the Brain Connectivity Toolbox, https://sites.google.com/site/bctnet/) to check whether a HFN can overcome the activity of other nodes of this biologically realistic network with higher degree. In figure 10 we show the network connectivity matrix (47 nodes, 505 links) (panel (a)) and the number of outgoing and incoming connections of each node (panel (b)). In panel (c) the network structure is depicted. Two nodes are highlighted for the following analysis: node 16 with an intermediate degree (outgoing (incoming) degree 7 (5)) and node 20 with a high degree of connectivity (outgoing (incoming) degree 23 (17)). The latter is considered a structural hub. Each of the 47 nodes is

ACCEPTED MANUSCRIPT

modeled, as in previous examples, with 80 excitatory and 20 inhibitory neurons with the same internal connectivity used in the previous simulations. The synaptic weights within the population are chosen as 0.2. The minimum synaptic weights between population are taken as 0.01. The rest of the weights are chosen as $g_{ij} = 0.01 dg_{max}/dg_i$ where g_{ij} is the connection weight from node j to node i, dg_{max} is the maximum in-degree of the network (in this case 23 which corresponds to the hub node number 6) and dg_i is the in-degree value of node i. To highlight our results, and without loss of generality, the outgoing synapses of nodes 16 and 20 are taken 0.1. Two periodic signals of amplitude 0.3 and frequencies $\omega_1 = 3.7$ Hz and $\omega_2 = 5.3$ Hz are applied on nodes 16^{th} and 20^{th}, respectively.

Initially, we look for the optimal frequency detuning ($\Delta\nu$) for which an external signal will better propagate in the network. In figure 11 we plot the response of the network, defined as the mean FFT amplitude of the firing rate of all nodes. In panels (a) and (b) it is clear that for node 16, $\Delta\nu = 2.4$ Hz optimizes the response while from panels (d) and (e) it is evident that $\Delta\nu = 3.6$ Hz optimizes the response of the network when node 20 is considered as HFN. The fact that different values of $\Delta\nu$ are optimum for different nodes is not surprising since the two nodes have a different degree of connectivity. When the two signals with $\omega_1 = 3.7$ Hz and $\omega_2 = 5.3$ Hz are applied on nodes 16^{th} and 20^{th}, respectively, their propagations strongly depend on the oscillating frequency of the host node. In panels (c) and (f) the time-delayed mutual information (δMI) of nodes 16 and 20 with all other nodes of the network is plotted for the optimum value of the inhomogeneity (which is $\Delta\nu = 2.4$ Hz for (c) and $\Delta\nu = 3.6$ Hz for (f)). Top/bottom figures of panels (c) and (f) show the δMI of node 16/20 to all other nodes of the network. Positive (negative) value of δMI indicates that the information preferentially flows in the outward (inward) direction of the node. In panel (c), when node 16 is the HFN, the δMI from node 16 to all other nodes, is almost always positive, confirming that the signal of 2.4 Hz propagates to all other nodes. Instead, the signal applied on node 20 propagates only to some of the nodes even though the node is a

ACCEPTED MANUSCRIPT

structural hub. In panel (f) we plot the δMI computed from node 16 and 20 when node 20 is the HFN. In the top panel, results indicate that δMI from node 16 is positive to some nodes and negative to others, indicating that it only effectively communicates with part of its target nodes. On the contrary, δMI from node 20 is positive to almost all nodes indicating that, in addition to being a structural hub, the high frequency further converts it in a functional hub.

Discussion

Propagation of signals in the nervous systems, either in the form of synfire propagation or rate propagation has been a core line of study in neuroscience in recent years (Vogels and Abbott (2005)). Several computational models have been proposed to guaranty reliability of the propagation of signals along with the prevention of the exploding activity in the network (Vogels and Abbott (2005); Kumar et al. (2010)). In this study, we showed that a heterogeneity in the firing rate of certain neuronal populations is enough to affect the propagation of signals in interconnected networks. Our main postulate is that each population is characterized by an endogenous collective oscillation whose frequency is the pivotal factor to determine the direction of signal propagation in the network. We showed that in a network with symmetric bidirectional connections, local perturbations on the dynamics of one node will propagate in the network, being detected by other nodes, if the node receiving the perturbation has a higher intrinsic frequency. In the same network, the perturbations on other nodes (with lower frequency), or perturbations on any site in a homogenous array where all the nodes oscillate with almost the same frequency, elicit no response in the nodes other than the host node. In such a network, the high frequency nodes seem to play the role of a *source* (Rubinov et al. (2011b)), being highly influential in activity propagation despite the symmetric homogeneous structure. Interestingly, it has been previously shown that high frequency units can suppress chaos and induce order (Braiman et al. (1995); Gavrielides et al. (1998); Valizadeh et al. (2010); Rajan et al. (2010)), and shape the structure of

ACCEPTED MANUSCRIPT

neural networks through synaptic plasticity (Bayati et al. (2015)).

Our results further show that slowly varying local signals can propagate along the network if the node that receives the input signal has a higher intrinsic firing rate. We showed that high frequency units determine the direction of signal propagation, so the effective connectivity in such a network. While structural network connections are bidirectional and symmetric, in the effective network the connections are directed outward from the high frequency node. Any population in this network can take the role of the source node in the effective network by increasing the frequency of its intrinsic oscillation. In this way, the effective connectivity can be changed on demand in a very simple and fast way by applying an extra control input on the population receiving the input signal, or by varying the strength of the existing inputs (e.g., by short- and long-term synaptic plasticity or neuromodulation). We envision source nodes as *functional hubs* whose capacity to influence activity propagation in the network is dynamically regulated, in opposition to classical (structural) hubs with rather fixed communication properties. Our simulations with heterogeneous networks, including the CoCoMac connectome network, confirm that high frequency nodes can act as functional hubs despite the presence of structural hubs in the network. In addition to this flexibility, it is important to note that transient source nodes can be also stabilized in certain conditions, in virtue of synaptic plasticity mechanisms introducing long-lasting changes in synaptic strengths. For instance, computational studies showed that through spike-timing-dependent plasticity, high frequency units can drive an initially symmetric structure into a feedforward network (Babadi and Abbott (2013); Jun and Jin (2007)). Also, the presence of a high frequency population in a locally connected random network has been shown to lead to the potentiation of the links outgoing from the high frequency neurons, and the depression of the incoming ones (Bayati et al. (2015)). Therefore, source nodes might regulate information flow at quite diverse time scales, as fast as firing rate can be regulated in a neuronal population by increasing their input, and as long lasting as synaptic potentiation can be durably changed in the network. Interestingly, experimental findings lend

ACCEPTED MANUSCRIPT

support to this hypothesis. fMRI studies in rodents have demonstrated that long-term potentiation of synaptic strength induced locally in the hippocampus, produce a functional reorganization of longer-range brain networks lasting several hours and shaping effective connectivity (Canals et al. (2009); Álvarez-Salvado et al. (2013)).

Which circuit elements and mechanisms underlay the influential capacity of source nodes? It has been hypothesized from experimental work that different phase relations between the rhythms generated by local sub-populations of neurons can control the routes of communication between brain areas (Fries (2005, 2015)). For appropriate phase relations, the spikes generated at a source area arrive at the target area in the time range over which the latter is highly excitable, e.g., when the inhibitory recurrent input within the target area is minimum (Fries (2009)). In our model, the response of the LIF neurons just after spiking is minimal and it increases exponentially with the phase (see Figure 3). For any two mutually coupled units in the $1:1$ locked mode, the phase of the unit with the larger intrinsic frequency advances that of the low frequency unit. So in every period, the spikes of the high-frequency node impact those of low frequency at the time when the target is highly excitable. Similarly, the spikes of the low-frequency unit have a small impact due to the low responsiveness of the high-frequency unit after firing.

Overall our study highlights a number of properties introduced by source nodes in networks with homogeneous connectivity. First, the influence of a node on the global dynamics not only depends on its position in the network nor its degree (Amit and Tsodyks (1992); Zbinden (2011)) but also on its internal dynamics, providing a fast and tunable mechanism to regulate information transmission. Second, source nodes transmit local information to distant nodes even in the absence of direct connections (polysynaptic propagation). This can reduce the wiring cost for effective long range connectivity (Laughlin et al. (1998); Bassett et al. (2010); Rubinov et al. (2011a)). Third, the high frequency unit introduces an effective direction for the transmission of information in the network, even in networks with symmetric connections. Fourth, our results rec-

ACCEPTED MANUSCRIPT

ommend the distinction between functional and structural hubs, and highlight that in heterogeneous network topologies structural hubs are not necessarily the most influential nodes.

Finally, it is worth mentioning that, although we presented results using a current-based leaky I&F model, qualitatively similar results were obtained with conductance-based leaky I&F model (see Supplementary Fig. S2), highlighting the wide validity of our findings. Despite the limitations of the model, the concepts and arguments of the present study can be used in a variety of systems of coupled oscillators to control the patterns of effective communication (see (Kirst et al. (2016))).

Acknowledgement

CRM acknowledge support from the Spanish Ministerio de Economía y Competitividad (MINECO) and Fondo Europeo de Desarrollo Regional (FEDER) through projects TEC2016-80063-C3-3-R (AEI/FEDER, UE). SC is supported by MINECO and FEDER funds under grants BFU2015-64380-C2-1-R and European Union Horizon 2020 research and innovation programme under grant agreement No 668863 (SyBil-AA). SC acknowledges financial support from the Spanish State Research Agency, through the Severo Ochoa Program for Centres of Excellence in R&D (SEV- 2013-0317).

References

Achard, S., Delon-Martin, C., Vértes, P.E., Renard, F., Schenck, M., Schneider, F., Heinrich, C., Kremer, S., Bullmore, E.T., 2012. Hubs of brain functional networks are radically reorganized in comatose patients, Proceedings of the National Academy of Sciences, 109(50). pp. 20608–20613.

Álvarez-Salvado, E., Pallarés, V., Moreno, A., Canals, S., 2013. Functional MRI of long-term potentiation: imaging network plasticity. Phil. Trans. R. Soc. B, 369. doi:10.1098/rstb.2013.0152.

ACCEPTED MANUSCRIPT

Amit, D.J., Tsodyks, M.V., 1992. Effective neurons and attractor neural networks in cortical environment. Network: Computation in Neural Systems, 3, 121–137.

Babadi, B., Abbott, L.F., 2013. Pairwise analysis can account for network structures arising from spike-timing dependent plasticity. PLoS Comput. Biol., 9. doi:10.1371/journal.pcbi.1002906.

Barabási, A.L., Albert, R., 1999. Emergence of scaling in random networks. Science, 286. doi:10.1126/science.286.5439.509.

Bassett, D.S., Greenfield, D.L., Meyer-Lindenberg, A., Weinberger, D.R., Moore, S.W., Bullmore, E.T., 2010. Efficient physical embedding of topologically complex information processing networks in brains and computer circuits. PLoS Comput. Biol., 6. doi:10.1371/journal.pcbi.1000748.

Bayati, M., Valizadeh, A., 2012. Effect of synaptic plasticity on the structure and dynamics of disordered networks of coupled neurons. Phys. Rev. E, 86, 011925.

Bayati, M., Valizadeh, A., Abbassian, A., Cheng, S., 2015. Self-organization of synchronous activity propagation in neuronal networks driven by local excitation. Front. Comput. Neurosci., 9. doi:10.3389/fncom.2015.00069.

Braiman, Y., Lindner, J.F., Ditto, W.L., 1995. Taming spatiotemporal chaos with disorder. Nature (London), 378.

Buckner, R.L., Sepulcre, J., Talukdar, T., Krienen, F.M., Liu, H., Hedden, T., Andrews-Hanna, J.R., Sperling, R., Johnson, K.A., 2009. Cortical hubs revealed by intrinsic functional connectivity: mapping, assessment of stability, and relation to alzheimer's disease. The Journal of Neuroscience, 29, 1860–1873.

Burkitt, A.N., 2006. A review of the integrate-and-fire neuron model: I. homogeneous synaptic input. Biol. Cybern., 95. doi:10.1007/s00422-006-0068-6.

ACCEPTED MANUSCRIPT

Canals, S., Beyerlein, M., Merkle, H., Logothetis, N.K., 2009. Functional MRI evidence for LTP-induced neural network reorganization. Curr. Biol., 19, 398–403.

Cortes, N., van Vreeswijk, C. 2015. Pulvinar thalamic nucleus allows for asynchronous spike propagation through the cortex. Frontiers in computational neuroscience, 9, 1-17.

Fornito, A., Zalesky, A., Pantelis, C., Bullmore, E.T., 2012. Schizophrenia, neuroimaging and connectomics. Neuroimage, 62, 2296–2314.

Fries, P., 2005. A mechanism for cognitive dynamics: neuronal communication through neuronal coherence. Trends Cogn. Sci., 9, 474–480.

Fries, P., 2009. Neuronal gamma-band synchronization as a fundamental process in cortical computation. Annu. Rev. Neurosci., 32. doi:10.1146/annurev.neuro.051508.135603.

Fries, P., 2015. Rhythms for cognition: Communication through coherence. Neuron, 88, 220–235.

Friston, K.J., 2011. Functional and effective connectivity: A review. Brain Connectivity, 1, 13–36. doi:10.1089/brain.2011.0008.

Fukushima, K., 2013. Artificial vision by multi-layered neural networks: neocognitron and its advances. Neural Network, 37, 103–119. doi:10.1016/j.neunet.2012.09.016.

Gavrielides, A., Kottos, T., Kovanis, V., Tsironis, G.P., 1998. Spatiotemporal organization of coupled nonlinear pendula through impurities. Phys. Rev. E, 58, 5529.

van den Heuvel, M.P., Sporns, O., 2013. Network hubs in the human brain. Trends in cognitive sciences, 17, 683–696. doi:10.1016/j.tics.2013.09.012.

ACCEPTED MANUSCRIPT

Jun, J.K., Jin, D.Z., 2007. Development of neural circuitry for precise temporal sequences through spontaneous activity, axon remodeling, and synaptic plasticity. PLoS ONE, 2. doi:10.1371/journal.pone.0000723.

Kawamura, Y., Nakao, H., Arai, K., Kori, H., Kuramoto, Y., 2008. Collective phase sensitivity. Phys. Rev. Lett, 101, 24101.

Kirst, C., Timme, M., Battaglia, D., 2016. Dynamic information routing in complex networks. Nature communications, 7. doi:10.1038/ncomms11061.

Kumar, A., Rotter, S., Aertsen, A., 2010. Spiking activity propagation in neuronal networks: reconciling different perspectives on neural coding. Nature Reviews Neuroscience, 11, 615–627. doi:doi:10.1038/nrn2886.

Laughlin, S.B., de R. van Steveninck, R.R., Anderson, J.C., 1998. The metabolic cost of neural information. Nature Neuroscience, 1.

Logothetis, N.K., 2012. Intracortical recordings and fMRI: an attempt to study operational modules and networks simultaneously. Neuroimage, 62, 962–969.

Park, H.J., Friston, K., 2013. Structural and functional brain networks: from connections to cognition. Science, 342.

Rajan, K., Abbott, L.F., Sompolinsky, H., 2010. Stimulus-dependent suppression of chaos in recurrent neural networks. Phys. Rev. E, 82, 011903.

Rubinov, M., Sporns, O., p Thivierge, J., Breakspear, M., 2011a. Neurobiologically realistic determinants of self-organized criticality in networks of spiking neurons. PLoS Comput. Biol., 7. doi:10.1371/journal.pcbi.1002038.

Rubinov, M., Sporns, O., Thivierge, J.P., Breakspear, M., 2011b. Neurobiologically realistic determinants of self-organized criticality in networks of spiking neurons. PLoS Comput. Biol, 7. doi:10.1371/journal.pcbi.1002038.

Sporns, O., 2014. Contributions and challenges for network models in cognitive neuroscience. Nature neuroscience, 17, 652–660.

ACCEPTED MANUSCRIPT

Valizadeh, A., Kolahchi, M.R., Straley, J.P., 2010. Single phase-slip junction site can synchronize a parallel superconducting array of linearly coupled Josephson junctions. Phys. Rev. B, 82, 144520.

Vogels, T.P., Abbott, L.F., 2005. Signal propagation and logic gating in networks of integrate-and-fire neurons. The Journal of Neuroscience, 25, 10786–10795.

Zbinden, C., 2011. Leader neurons in leaky integrate and fire neural network simulations. J. Comput. Neurosci, 31, 285–304.

ACCEPTED MANUSCRIPT

ACCEPTED MANUSCRIPT

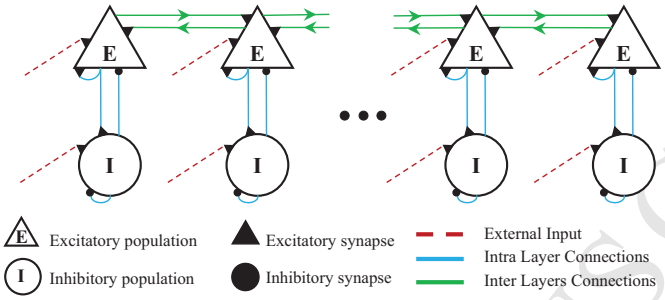

Figure 1: **Network configuration.** The network is composed of 11 neuronal layers (or nodes), each containing 80 excitatory (triangles) and 20 inhibitory (circles) neurons. Neurons within the nodes are randomly connected to each other with probability 0.1. Excitatory neurons of adjacent nodes are mutually connected with 0.1 probability (green arrows).

ACCEPTED MANUSCRIPT

ACCEPTED MANUSCRIPT

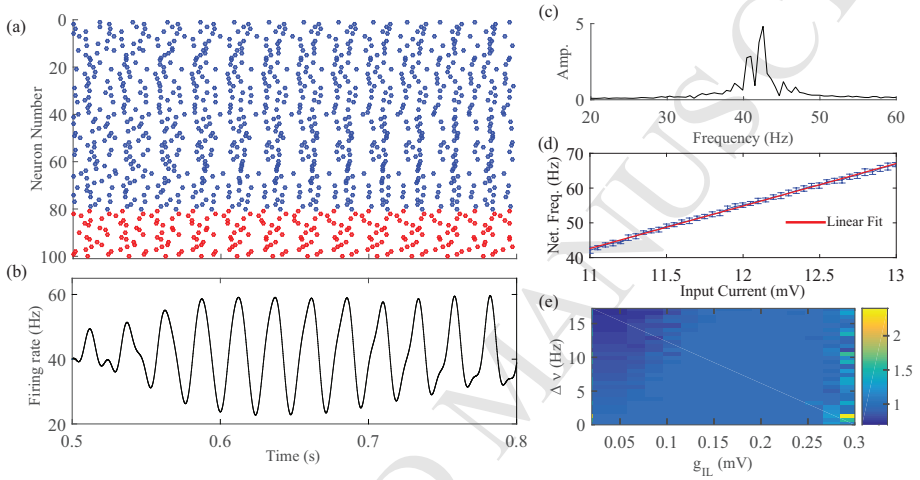

Figure 2: **Network dynamics and locking region.** (a) Characteristic raster-plot of the spiking activity of an isolated node. Blue (Red) dots represent Excitatory (Inhibitory) neurons. (b) Mean firing rate of the excitatory neurons of an isolated node (i.e., in the absence of inter-node connections). The power spectrum of the node shown in (c) shows an activity in the gamma range whose frequency $\nu_0 \sim 42$ Hz can be controlled by the external current as it is shown in panel (d). Panel (e) shows the frequency difference between two adjacent nodes (in this case 5 and 6) for an increasing value of the inter-node connection strength (g_{IN}). The region with light blue color indicates that the populations are locked in the $1:1$ regime, i.e., they oscillate at the same frequency.

ACCEPTED MANUSCRIPT

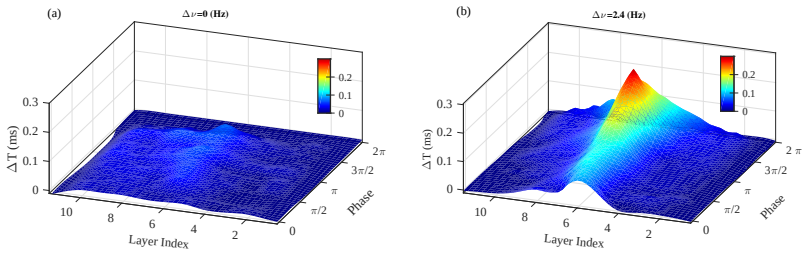

Figure 3: **Spatio-temporal response of the network.** (a) In a homogeneous network where $\Delta\nu = 0$, i.e., all nodes oscillate at the frequency $\approx \nu_0 \sim 42$ Hz, the response function is negligible small and, as expected, independent of the location of the host node and phase at which the current pulse is injected. (b) In the presence of a high-frequency node (with $\nu = \nu_0 + \Delta\nu = 44.4$ Hz) the response critically depends on the location of the node that receives the input and phase at which the current pulse is injected. The response sharply decays when the host node is moved away from the high frequency node and the phase moves away from $\sim \frac{3}{2}\pi$. The network consists of 11 nodes and the 6^{th} node is the high frequency node in panel (b).

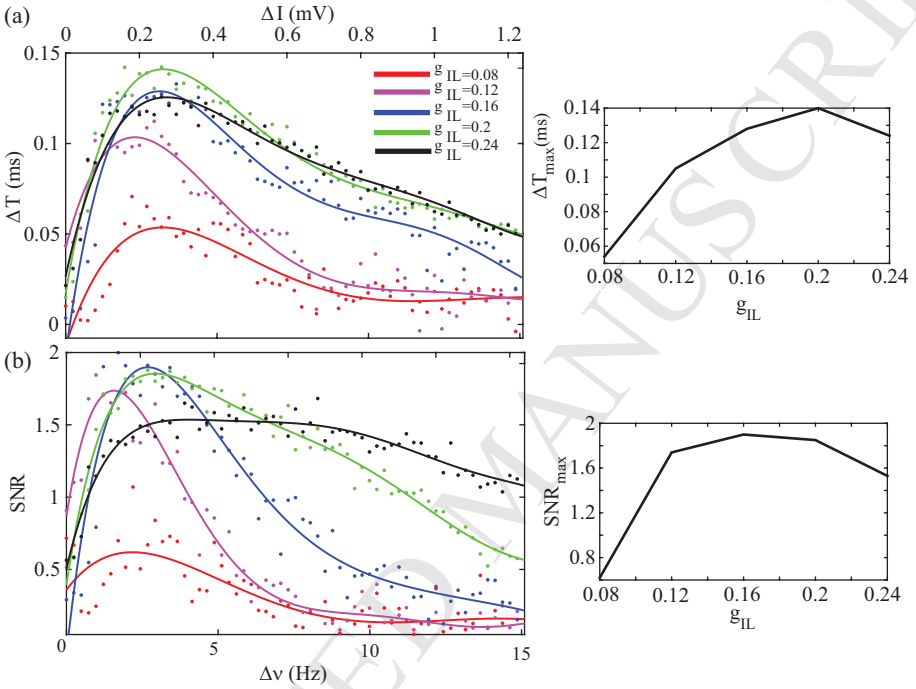

Figure 4: **Dependence of the response on the level of inhomogeneity** (a) Mean response of the network and (b) SNR (mean value normalized to the standard deviation) are plotted vs. the inhomogeneity parameter ΔI (or equivalently the oscillation frequency mismatch $\Delta\nu$, see Figure 2 (d)) for different values of the inter-node (IN) synaptic strength g_{IN}. Both measures show that an optimum response is attained for a relatively small value of $\Delta\nu$. In the right panels of (a) and (b) the maximum values of the mean response and the SNR are plotted versus the inter-node connection strengths. The results were obtained averaging over 500 trials. Dots in (a) and (b) show the simulation data and lines are the result of a polynomial fit.

ACCEPTED MANUSCRIPT

ACCEPTED MANUSCRIPT

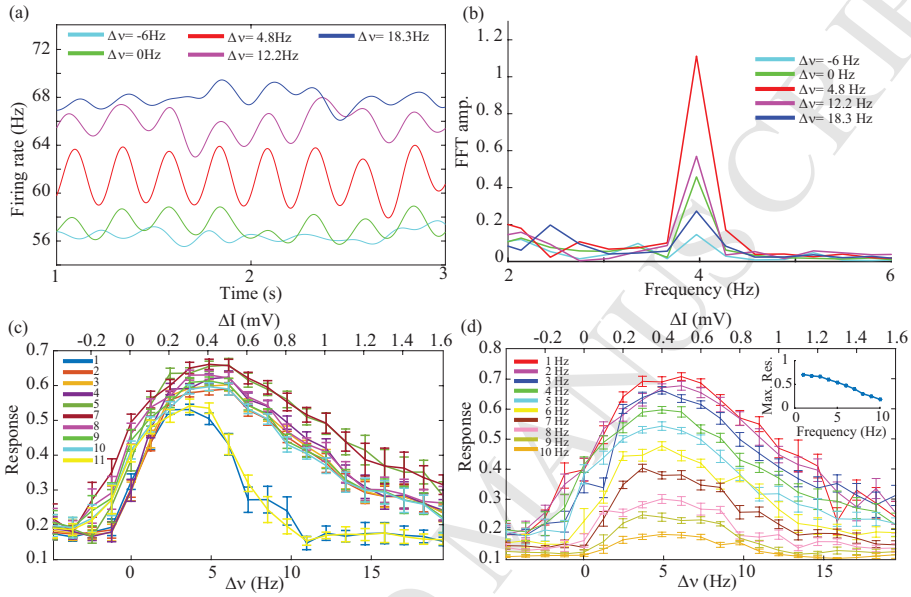

Figure 5: **Response of the network to a local periodic signal.** (a) The mean firing rate of a sample node (node 10) is plotted for different inhomogeneity values in the middle node (node 6). The population rate is calculated over a Gaussian time window of 50 ms width. The amplitude of the external sinusoidal signal is 0.5 mV and its frequency $f_0 = 4$ Hz (see Material and Methods section). (b) The Fourier amplitude of the population rate is plotted for several $\Delta\nu$ values. It can be seen that the height of the Fourier transform at the frequency of the external signal depends on the inhomogeneity value. (c) Cross covariance between all nodes calculated at the frequency of the external signal f_0=4 Hz as a function of $\Delta\nu$ (equivalently ΔI in the upper axis). Colors indicate the node number. The maximum response of the network is found for an intermediate value of $\Delta\nu \sim 5$ Hz ($\Delta I \simeq 0.4$ mV). (d) The response of a sample node (node 10) vs. the inhomogeneity parameter $\Delta\nu$ is plotted for several values of the frequency of the external signal f_0 (from 1 to 10 Hz). The maximum response decreases for higher frequencies as is shown in the inset.

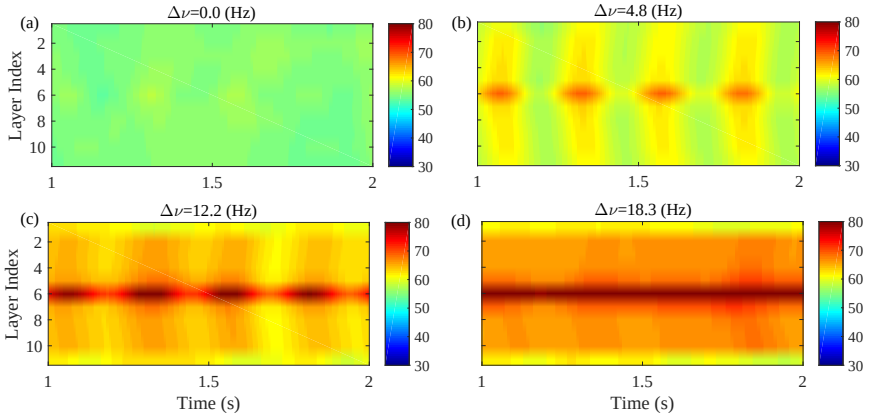

Figure 6: **Response of the network to an external signal.** The firing rate of all the nodes in the array is shown for several values of the inhomogeneity parameter ($\Delta\nu$ =0, 4.8, 12.2, and 18.3 Hz). A clear propagation of the signal from the middle node to other nodes is seen for $\Delta\nu = 4.8$ Hz. Colors code represents the mean activity of the nodes which is calculated over a Gaussian time window of width 50 ms.

ACCEPTED MANUSCRIPT

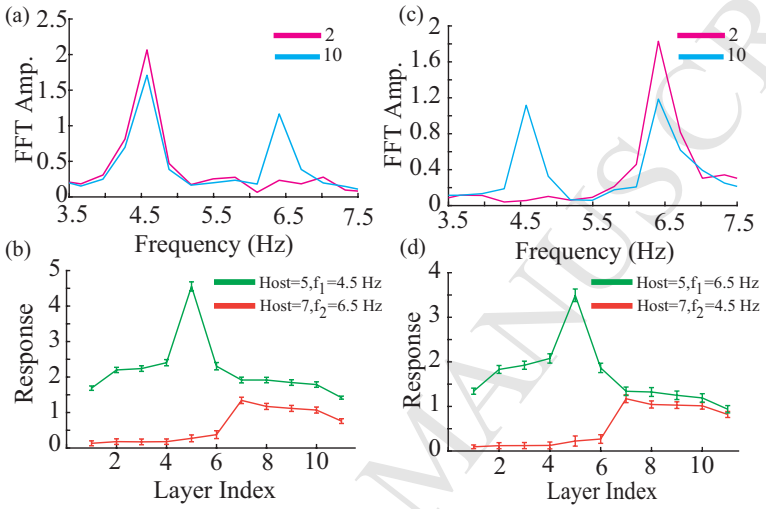

Figure 7: **Effective connectivity is determined by the high frequency node.** To reveal the effective connectivity in the network in the presence of a high frequency node (node 5), we inject two periodic signals. One signal with frequency f_1 is injected into the high-frequency node 5 and another signal with frequency f_2 into another node of oscillating frequency ν_0 (in this case node 7). (a) Power spectra of the activity of nodes 2 and 10. While the signal applied to the high-frequency node is received by the two sampled nodes, the signal applied to the low frequency node only reaches node 2, which is located to the left of the high frequency node. (b) Response of all the nodes to a signal with frequencies f_1 (f_2) applied to node 5 (7). The green curve indicates that the signal of frequency f_1 reaches all nodes while the signal of frequency f_2 (red curve) only propagates in the direction away of the high-frequency node. Results presented in panels (c) and (d) are similar to those presented in panels (a) and (b) but with the external signal frequencies interchanged (see legends).

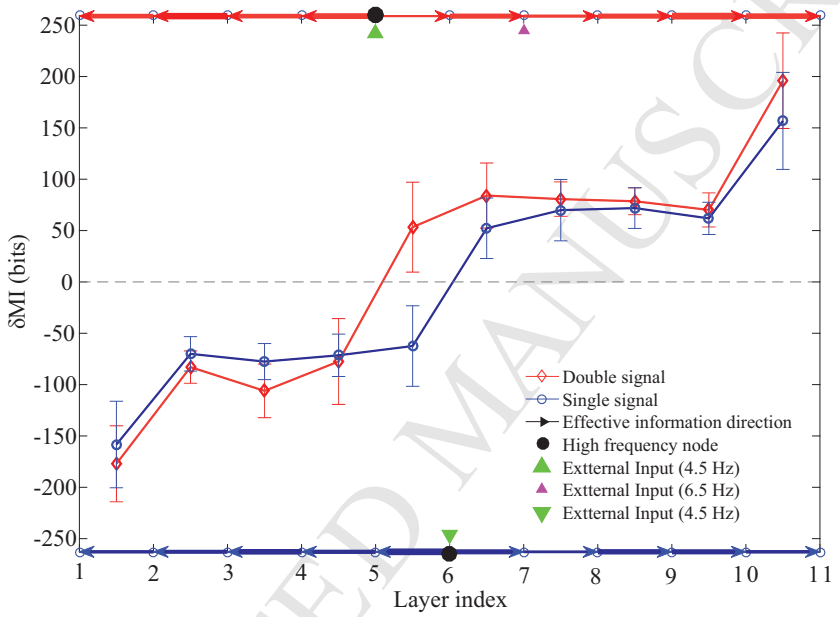

Figure 8: **Difference δMI transfer in a chain of nodes (δMI).** Information flow, computed via the difference of the delayed-mutual information index, in a chain of 11 nodes. Red curve corresponds to the δMI computed when two signals with frequencies 4.5 and 6.5 Hz are applied simultaneously on nodes 5 (the high-frequency node (HFN) and 7, respectively. The blue curve corresponds to the δMI computed for one signal with frequency 4.5 applied on the HFN (in this case node 6). In both cases, the flow of information is such that it moves away from the HFN. The frequency of HFN node is $\nu = \nu_0 + \Delta\nu = 46.8$ Hz.

ACCEPTED MANUSCRIPT

ACCEPTED MANUSCRIPT

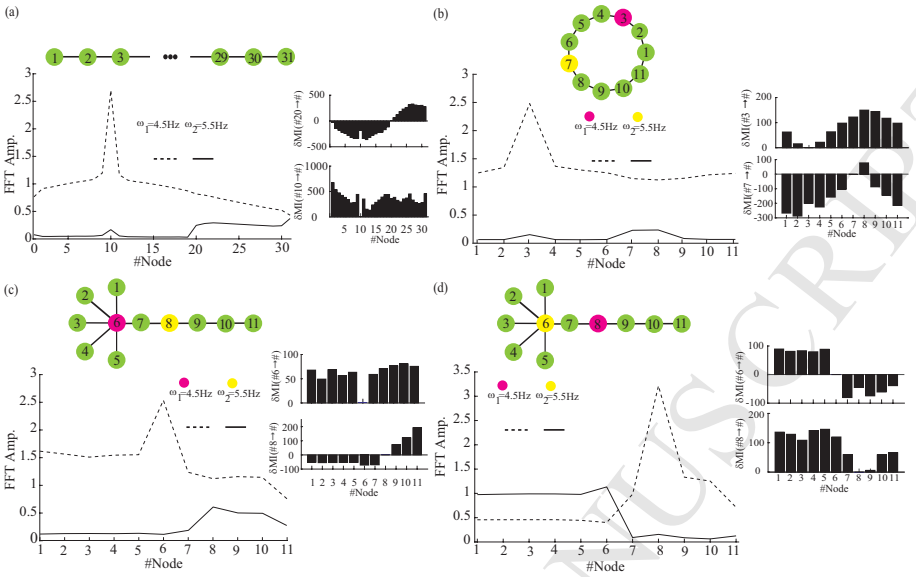

Figure 9: **Response of nodes in different topologies.** Results are shown for the optimum value of the frequency of the HFN, in this case $\nu = \nu_0 + \Delta\nu \sim 49.3$ Hz. The barplot in the right of each panel shows the δMI of two selected nodes with all the other nodes. Positive (Negative) value of δMI for the nodes X and Y shows that the information propagated from X to Y (from Y to X). (a) Response of a chain composed by 31 nodes subject to two signal. As occurs for the case of less number of nodes, the signal applied on the HFN (node 10) propagates along the whole chain (dashed line) while that applied to a normal node (node 20; solid line) only propagates in the direction away from the HFN. The inter-node synaptic weights are 0.2. In panel (b) we plot the response of the nodes in a ring configuration (11 nodes) when two signals are applied at the 3^{rd} (the HFN) and 7^{th} nodes. The signal applied on HFN node is detected by all other nodes, while the signal applied at the 7^{th} node fades away. The inter-node synaptic weights are 0.2. (c) Combination of a starlike and a chain configuration. The network has a structural hub (6^{th}) node, which is connected to nodes 1 to 5 and 7. In this panel, the HFN is node 6. Signals are applied to nodes 6 and 8. While the signal applied at the HFN reaches the whole network, the one applied at node 8 only propagates away from the HFN. The inter-node synaptic weights from node 6 to nodes 1-7 are 0.05 and from nodes 1-5,7 to node 6, 0.25. For the rest of the nodes, the inter-node synaptic weights are 0.2. When the HFN is not the structural hub (panel d) the signal applied at the HFN (node 8) propagates along the whole network (including the star). However, the signal applied at the structural hub (node 6, oscillating at frequency ν_0) can only propagate to the nearest neighbors since it is blocked by the HFN. The inter-node synaptic weights form nodes 1-5 to 6 are 0.04, from 7 to 6 0.12 and from 6 to the others 0.25. For the rest of the nodes, the inter-node synaptic weights are 0.2.

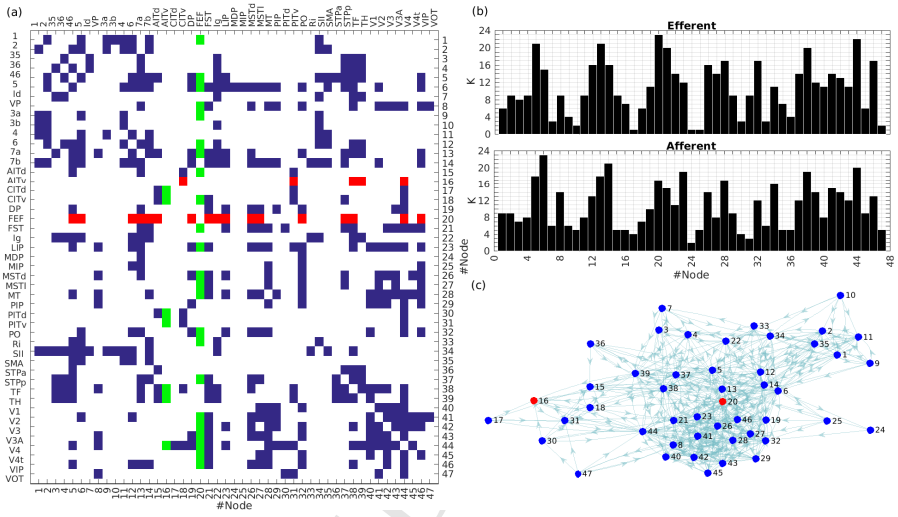

Figure 10: **Macaque connectome details.** (a) Adjacency matrix of Macaque connectome (N=47, K=505). Each dark square shows presence of a connection between regions with labels given in top x- and left y-axis. To address the node through the text we use the corresponding labels in bottom x- and right y-axis. (b) Top/Bottom panel shows the number of outgoing/incoming connections of each node to/from other nodes. (c) Graphical representation of the connectome network. The two red circles (node 16 with an intermediate degree and node 20 which is a structural hub) are the nodes that we chose to study the signal propagation.

ACCEPTED MANUSCRIPT

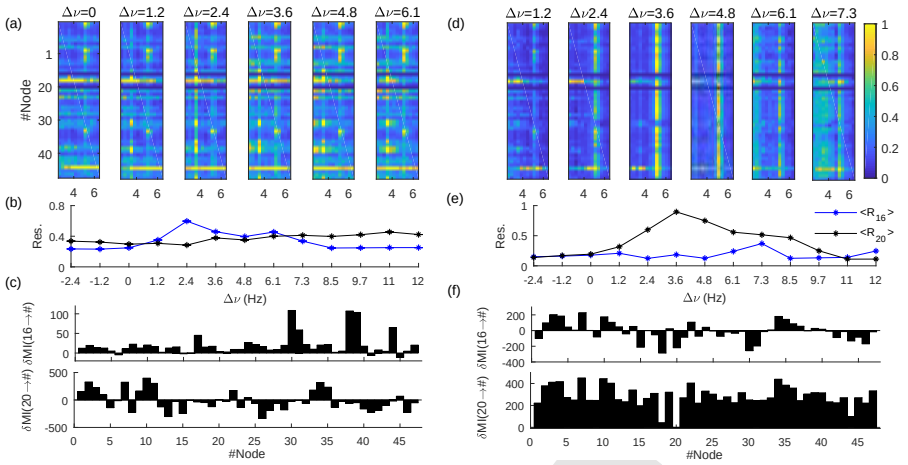

Figure 11: **Double signal propagation in Macaque47 connectom.** Two signal with $\omega_1 = 3.7$ Hz and $\omega_2 = 5.3$ Hz are applied on nodes 16^{th} and 20^{th}, respectively. In left panels (a-c) the 16^{th} node is the HFN while the hub, 20^{th} node, oscillates with the same average frequency of the other nodes. In right panels (d-f) the node 16^{th} is a normal node while the node 20^{th} is the HFN as well as the hub. In panels (a) and (d) we plot the FFT amplitude of the firing rate of all the nodes. The FFT amplitude of node 16 and 20 are discarded in the representation for the sake of better clarity of the figures. In (b) and (e) the mean of FFT amplitude of the firing rate of all the nodes at the signal frequency applied on nodes 16 (blue line) and 20 (black line) are plotted versus the inhomogeneity $\Delta\nu$ when the activity of the directly connected nodes to node 16 and 20 are excluded. In (c) and (f) the time-delayed mutual information δMI of nodes 16 and 20 with all nodes of the network is plotted at the optimum value of their inhomogeneities ($\Delta\nu = 2.4$ Hz for node 16 and $\Delta\nu = 3.6$ Hz for node 20). Top/bottom panels show the δMI of node 16/20 to all other nodes of the network. Positive/Negative values of δMI indicate that the information flow is in the outward/inward direction from/to the node. In (c) the outgoing δMI of node 16 is positive at almost every node indicating that the information propagates outward from node 16 to all other nodes. On the contrary, the information generated in node 20 propagates only to some of the nodes. In (f) the outgoing δMI of node 16 is positive for some nodes and negative for others, indicating that it sends/receives information to/from other nodes. The δMI measured from the signal generated at node 20 is positive to almost all other nodes indicating that this node is not only a structural hub but also a functional hub.